Theory of antiferromagnetic superlattices at finite temperatures

H. T. Diep*
Fundamental Research Laboratories, NEC Corporation, 4-1-1 Miyazaki, Miyamae-ku, Kawasaki 213, Japan
(Received 3 April 1989)

Magnetic properties of antiferromagnetic superlattices at finite temperatures are investigated theoretically by a multisublattice Green-function technique which takes into account the quantum nature of Heisenberg spins. The results of various physical quantities and the magnetic transition temperature are shown for different sets of intraplane and interplane interactions. In particular, in the case of stacking of alternative weak and strong layers, we find a crossover between layer magnetizations due to quantum fluctuations at low temperatures, which has no counterpart in ferromagnetic superlattices. Monte Carlo simulations of the corresponding classical Heisenberg model spins have also been carried out, and a comparison between the two methods is given.

I. INTRODUCTION

Magnetic superlattices have been extensively studied in the past decade. Experimentally, successful growth and characterization of magnetic superlattices by advanced techniques have been realized. In particular, magnetic superlattices Dy/Y have been obtained by molecular-beam epitaxy,[1] and superlattices of transition metal and Mg have been fabricated by magnetron sputtering.[2] In general, small magnetizations and lower magnetic transition temperatures with respect to the bulk values have been observed. Theoretically, many investigations on magnetic superlattices have been done with different models and methods. Dobrzynski and co-workers have studied, by a Green-function technique, the bulk and surface magnons in a Heisenberg ferromagnetic superlattice consisting of two semi-infinite films,[3] and in a ferromagnetic film sandwiched between two different semi-infinite ferromagnets.[4] Lin and coworkers[5,6] have investigated magnetic excitations of a Heisenberg ferromagnetic superlattice consisting of alternative layers of A and B atoms, by a local density of magnon states,[5] and by a Green-function method.[6] A similar system has been studied by Schwenk *et al.*[7] using a Ginzburg-Landau analysis. On the other hand, Camley *et al.*[8] have investigated spin waves and the light-scattering spectrum of a system consisting of alternative ferromagnetic and nonmagnetic films, taking into account the Zeeman and dipolar interactions but neglecting exchange. Similar systems were also studied by other authors.[9] Hillebrands[10] later generalized these systems to take into account the exchange and surface anisotropy contributions. Hinley and Mills[11] have studied systems formed by alternative Heisenberg ferromagnetic and antiferromagnetic films, using a classical ground-state analysis and a spin-wave theory. Other studies of superlattices include the works by Thibaudeau and Caillé[12] and by Zhou and Gong[13] who investigated magnetic polaritons in systems of magnetic layers separated by dielectric layers. Finally, systems consisting of alternative layers of Ising and Heisenberg spins were investigated by Valadares and Plascak,[14] and quasiperiodic ferromagnetic superlattices were also probed by Pang and Pu.[15]

To our knowledge, at present there has not been investigation on antiferromagnetic superlattices at finite temperatures. The above-mentioned works have dealt exclusively with the zero-temperature properties (except Ref. 6) and with ferromagnetic superlattices (except Ref. 8). This defines the purpose of the present work.

The aim of this paper is (i) to work out a general Green-function formalism to study the critical temperature and properties of magnetic superlattices with quantum Heisenberg spins at finite temperatures, (ii) to apply the formalism to a few examples of antiferromagnetic superlattices, and (iii) to simulate by Monte Carlo (MC) technique the same model with classical Heisenberg spins in order to compare with the quantum case.

Section II is devoted to the Green-function formalism. Although the equations shown are derived for the case of binary antiferromagnetic superlattices consisting of stacked layers of square lattices for the sake of concreteness, the formalism can be generalized to include systems such as antiferromagnetic superlattices of three or more different kinds of layers and other lattice structures. Applications are shown and discussed in Sec. III. Results of MC simulations are presented and compared to the quantum case in Sec. IV. Concluding remarks are given in Sec. V.

II. GREEN-FUNCTION METHOD

We consider the following Hamiltonian

$$H = 2\sum_{ij} J_{ij}\mathbf{S}_i\cdot\mathbf{S}_j + 2D\sum_{ij} S_i^z S_j^z \ , \tag{1}$$

where J_{ij} is the exchange integral between two spins S_i and S_j at the lattice sites i and j, respectively. All interactions J_{ij} are assumed to be antiferromagnetic (>0), but with different magnitudes. D denotes an anisotropy introduced for numerical calculation convenience but having a microscopic origin. D is small and therefore assumed to be site independent. Let us define the z axis to be perpendicular to the layers A and B. When D is negative the spins lie in the planes A and B, and when D is

positive, the spins will be directed in the $+z$ or $-z$ directions. Anisotropy of the latter kind of found, for example, in compounds of Cu^{2+} with spins one-half.[16] Hereafter, D is assumed to be positive for simplicity.

Let us consider a four-sublattice model in this section, although the formalism presented here can be generalized to many-sublattice models as seen later on. In the four-sublattice model, the exchange interactions in the A and B planes are denoted by J_A and J_B, respectively, and the interplane interactions between neighboring spins on two adjacent A and B planes are J_{AB} (see Fig. 1). By magnetic symmetry, there are two sublattices corresponding to up and down spins for the A planes and two other ones for the B planes.

Following Zubarev,[17] we define a double-time Green function by

$$G_{ij}(t,t')=\langle\langle S_i^+(t);S_j^-(t')\rangle\rangle \ . \tag{2}$$

The equation of motion for $G_{ij}(t,t')$ reads

$$i\,dG_{ij}/dt=\langle[S_i^+(t),S_j^-(t')]\rangle\delta(t-t') - \langle\langle[H,S_i^+(t)];S_j^-(t')\rangle\rangle \ , \tag{3}$$

where $\delta(t-t')$ is the Dirac delta function, $\langle\ldots\rangle$ means the thermal average, and $\hbar=1$ has been used. The second term on the right-hand side of Eq. (3) will generate different kinds of Green functions of lowest order defined by (3) as well as higher-order Green functions. The latter can be reduced to lowest-order Green functions by using the so-called Tyablikov decoupling scheme, for example

$$\langle\langle S_i^z S_i^+(t);S_j^-(t')\rangle\rangle \cong \langle S_i^z\rangle\langle\langle S_i^+(t);S_j^-(t')\rangle\rangle \ . \tag{4}$$

Due to the symmetry, there are four Green functions for the four-sublattice model considered here, namely two of the type $G_{ij}(t,t')$ where i and j belong to the same sublattice (one for layer A and one for layer B), and two of the type $F_{ij}(t,t')$ where i and j belong to different sublattices as seen explicitly in the following. Furthermore, to emphasize the layered structure we shall use first the following Fourier transform in the xy plane

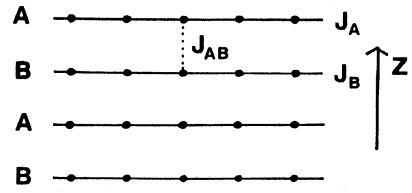

FIG. 1. Side view of binary superlattice with alternative layers of A and B atoms stacked in the stacked in the z direction. Intraplane interactions are denoted by J_A and J_B, and interplane interaction by J_{AB}.

$$H_{ij}(t,t')=(1/\pi^2)\int\int dk_x dk_y \left[\frac{1}{2\pi}\right] \times\int d\omega\, H_{nm}(\omega,k_x,k_y) \times\exp[-i\omega(t-t')] \times\exp[i\mathbf{k}_{\parallel}\cdot(\mathbf{r}_i-\mathbf{r}_j)] \ , \tag{5}$$

where $H_{ij}(t,t')$ stands for any of the four Green functions previously defined, $\mathbf{k}_{\parallel}$ is a wave vector parallel to the xy plane, ω is a spin-wave eigenfrequency, and n and m denote the z components of the positions of the spins $\mathbf{r}_i$ and $\mathbf{r}_j$, i.e., indices of the layers to which $\mathbf{r}_i$ and $\mathbf{r}_j$ belong, respectively. Assuming that the nth layer is of the A type and the $(n+1)$th layer is of the B type, one obtains the following set of equations:

$$(E-A_n)g_{nn'}=2\mu_n\delta_{nn'}+B_n f_{nn'}+C_n(f_{n+1,n'}+f_{n-1,n'}) \ , \tag{6a}$$

$$(E+A_n)f_{nn'}=-B_n g_{nn'}-C_n(g_{n+1,n'}+g_{n-1,n'}) \ , \tag{6b}$$

$$(E-A_{n+1})g_{n+1,n'}=2\mu_{n+1}\delta_{n+1,n'}+B_{n+1}f_{n+1,n'}+C_{n+1}(f_{n+2,n'}+f_{nn'}) \ , \tag{6c}$$

$$(E+A_{n+1})f_{n+1,n'}=-B_{n+1}g_{n+1,n'}-C_{n+1}(g_{n+2,n'}+g_{nn'}) \ , \tag{6d}$$

where the following notations have been used:

$$E=\omega/J_A,\ g_{nn'}=J_A G_{nn'},\ f_{nn'}=J_A F_{nn'} \ ,$$

$$g_{n+1,n'}=J_A G_{n+1,n'},\ f_{n+1,n'}=J_A F_{n+1,n'} \ ,$$

$$A_n=2(1+d)(4\mu_n+\epsilon\mu_{n+1}+\epsilon\mu_{n-1}) \ ,$$

$$A_{n+1}=2(1+d)(4\alpha\mu_{n+1}+\epsilon\mu_{n+2}+\epsilon\mu_n) \ ,$$

$$B_n=8\mu_n\gamma \ ,$$

$$B_{n+1}=8\alpha\mu_{n+1}\gamma \ ,$$

$$C_n=2\epsilon\mu_n \ ,$$

$$C_{n+1}=2\epsilon\mu_{n+1} \ ,$$

$$\epsilon=J_{AB}/J_A \ ,$$

$$\alpha=J_B/J_A \ ,$$

$$d=D/J_A \ ,$$

$$\gamma=\cos(k_x a/2)\cos(k_y a/2) \ ,$$

a being the in-plane lattice constant, and

$$\mu_n=|\langle S_i^z\rangle| \ ,$$

i belonging to the nth layer.

It is worth noting at this stage that one can easily generalize the set of equations (6) to the case of the six-sublattice model consisting of three different magnetic layers in the unit cell in the z direction, namely A, B, and

C. In that case, one has to write two other equations for the $(n+2)$th layer and one obtains a set of six equations instead of four. Thus, the interest of expressing the Green functions under the form (6) is to elicit the layer character of this system. In the case of thin films, one just has to modify the conditions at the surfaces. Our previous work on single thin films[18,19] has shown that this method is powerful for investigating finite-temperature behavior including the magnetic transition.

Now, taking the advantage that the system is periodic with two lattice spacings in the z direction, one introduces the following plane waves:

$$f_{n-1}=f_{n+1}\exp(-ik_z c)\ ,$$

$$g_{n-1}=g_{n+1}\exp(-ik_z c)\ ,$$

where c is the lattice periodicity in the z direction. The set of equations (6) is now readily rewritten under the following matrix form:

$$\mathbf{Mg}=\mathbf{u}\ , \tag{7}$$

where

$$\mathbf{M}=\begin{bmatrix} E-A_n & -B_n & 0 & -Z_n \\ B_n & E+A_n & Z_n & 0 \\ 0 & -Z_{n+1}^* & E-A_{n+1} & -B_{n+1} \\ Z_{n+1}^* & 0 & B_{n+1} & E+A_{n+1} \end{bmatrix}\ , \tag{8}$$

$$\mathbf{g}=\begin{bmatrix} g_{nn'} \\ f_{nn'} \\ g_{n+1,n'} \\ f_{n+1,n'} \end{bmatrix}\ , \tag{9a}$$

$$\mathbf{u}=\begin{bmatrix} 2\mu_n\delta_{nn'} \\ 0 \\ 2\mu_{n+1}\delta_{n+1,n'} \\ 0 \end{bmatrix}\ , \tag{9b}$$

$$Z_n=2\epsilon\mu_n[1+\exp(-ik_z c)]\ ,$$

$$Z_{n+1}=2\epsilon\mu_{n+1}[1+\exp(-ik_z c)]\ ,$$

and Z^* is the complex conjugate of Z.

The case of an isotropic simple-cubic antiferromagnet (one kind of exchange interaction) can be recovered by noticing that there are only two sublattices which allow one to write

$$h_{n\pm1,n'}=h_{nn'}\exp(\pm ik_z a)\ ,$$

where h stands for g and f. One then has only two coupled equations with $g_{nn'}$ and $f_{nn'}$ whose secular equation yields the well-known spin-wave spectrum of the simple-cubic antiferromagnet

$$E_k=\pm 12\mu[(1+d)^2-\gamma_k^2]^{1/2}\ ,$$

where

$$\gamma_k=[\cos(k_x a)+\cos(k_y a)+\cos(k_z a)]/3\ .$$

The spin-wave spectrum of the four-sublattice model is easily obtained by solving the secular equation of the set of equations (6). Though complex, it gives four real solutions which are

$$E_k=\pm\{0.5[P\pm(P^2-4Q)^{1/2}]\}^{1/2}\ , \tag{10}$$

where

$$P=-A_{n+1}^2+B_{n+1}^2-A_n^2+B_n^2+2Z_{n+1}^*Z_n\ ,$$

and

$$\begin{aligned} Q=&(-A_{n+1}^2+B_{n+1}^2)(-A_n^2+B_n^2) \\ &-2A_nA_{n+1}Z_nZ_{n+1}^* \\ &-2B_nB_{n+1}Z_nZ_{n+1}^*+Z_n^2Z_{n+1}^{*2}\ . \end{aligned}$$

These four solutions will be denoted hereafter as E_k^i $(i=1-4)$. E_k^i relates the neighboring layer magnetizations μ_n, μ_{n+1}, and μ_{n-1}. Now, using the spectral theorem[12] which relates the correlation function $\langle S_i^+S_j^-\rangle$ to the Green functions, one has

$$\begin{aligned} \mu_m=\langle S_m^z\rangle&=\tfrac{1}{2}-\langle S_m^+S_m^-\rangle \\ &=\tfrac{1}{2}-\lim_{\xi\to0}(1/\pi^3)\int\int\int d\mathbf{k}\int dE_k(i/2\pi) \\ &\quad\times[g_{mm}(E_k+i\xi)-g_{mm}(E_k-i\xi)] \\ &\quad\times[\exp(E_k/\theta)-1]^{-1}\ , \end{aligned} \tag{11}$$

where m stands for n and $n+1$, i on the third equality is the imaginary number, and $\theta=k_BT/J_A$. From (7), one has

$$g_{mm}(E_k)=|\Delta_{mm}(E_k)|/|\Delta(E_k)|\ , \tag{12}$$

where $|\Delta(E_k)|$ is the determinant of $\mathbf{M}$ and $|\Delta_{mm}(E_k)|$ is obtained from $|\Delta(E_k)|$ by replacing the first (if $m=n$) or the third (if $m=n+1$) column by (9b), taking $n'=m$. Writing $|\Delta(E_k)|=\prod_i(E-E_k^i)$ $(i=1-4)$, one can express g_{mm} as

$$g_{mm}(E)=\sum_i a_m(E_k^i)/(E-E_k^i)\quad(i=1-4)\ , \tag{13}$$

where it is easy to show that

$$a_m(E_k^i)=|\Delta_{mm}(E_k)|/\prod_j(E_k^i-E_k^j),\quad\text{with } j\neq i\ .$$

Using (12) and the relation

$$1/(x-i\xi)-1/(x+i\xi)=2\pi i\delta(x)\ ,$$

i being the imaginary number, one finally obtains

$$\mu_n=\tfrac{1}{2}-(1/\pi^3)\int\int\int d\mathbf{k}\sum_i a_n(E_k^i)[\exp(E_k^i/\theta)-1]^{-1}\ , \tag{14a}$$

$$\mu_{n+1}=\tfrac{1}{2}-(1/\pi^3)\int\int\int d\mathbf{k}\sum_i a_{n+1}(E_k^i)\times[\exp(E_k^i/\theta)-1]^{-1}\ . \tag{14b}$$

Equations (14) couple the magnetizations of three neighboring layers via E_k^i [see Eq. (10)]. However, for the binary structure considered here, one has by symmetry $\mu_{n-1}=\mu_{n+1}$; therefore, there are only two equations (14a) and (14b) for μ_n and μ_{n+1} to be solved self-consistently.

The layer magnetizations at zero temperature are given by

$$\mu_n^0=\tfrac{1}{2}+(1/\pi^3)\int\int\int d\mathbf{k}\sum_i a_n(E_k^i)\ , \tag{15a}$$

$$\mu_{n+1}^0=\tfrac{1}{2}+(1/\pi^3)\int\int\int d\mathbf{k}\sum_i a_{n+1}(E_k^i)\ , \tag{15b}$$

where the sums run over only negative values of E_k^i. These equations allow us to estimate the zero-point spin contractions in a self-consistent manner.

The Néel temperature T_N can be obtained by setting μ_n and μ_{n+1} on the left-hand sides of the two equations (14) to zero and using

$$\exp(E_k^i/\theta)-1\simeq E_k^i/\theta_N(\theta_N=k_B T_N/J_A)$$

as $T\to T_N$. These two equations give two following equations which determine T_N self-consistently:

$$\theta_N^{-1}=(2/\pi^3)\int\int\int d\mathbf{k}\sum_i[a_n(E_k^i)/E_k^i]\quad(i=1\text{–}4)\ , \tag{16a}$$

$$\theta_N^{-1}=(2/\pi^3)\int\int\int d\mathbf{k}\sum_i[a_{n+1}(E_k^i)/E_k^i]\quad(i=1\text{–}4)\ . \tag{16b}$$

In the case where $\alpha=1$, one has $\mu_n=\mu_{n+1}=\mu$; the quantities in the square brackets tend to a finite value [the coefficients a_n, a_{n+1}, and E_k^i are proportional to μ, therefore the right-hand sides of (16) are in fact independent of μ]. In the case where $\alpha\neq 1$, μ_n and μ_{n+1} do not tend to zero in the same manner at T_N; however, the quantities in the square brackets still tend to a finite value which has to be determined self-consistently.

III. APPLICATIONS

Numerical calculations have been carried out for different sets of parameters ϵ, α, and d. To calculate the layer magnetizations at a given temperature, guessed values for μ_n and μ_{n+1} are used to calculate the spin-wave spectrum E_k [Eq. (10)] which is then used to calculate μ_n and μ_{n+1} by (14). An iteration procedure is used until a self-consistent solution for μ_n and μ_{n+1} at each given temperature is obtained. In doing so, one obtains also the self-consistent temperature dependence of the spin-wave spectrum. A total of 40^3 points were taken in the first Brillouin zone. At low temperatures, a few iterations suffice to get a precision of 0.1%. In the following we show the results for some special cases taking $d=0.1$. The effect of d will be shown later.

A. $\epsilon<1$, $\alpha=1$

This case simulates a system which consists of identical layers separated by nonmagnetic layers. The interactions between the spins via the nonmagnetic layer are weakened ($\epsilon<1$). It can also be viewed as a quasi-two-dimensional system. By symmetry, one has $\mu_n=\mu_{n+1}=\mu$.

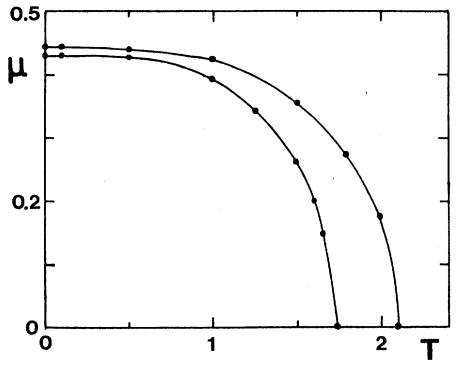

FIG. 2. Layer magnetization μ vs temperature T for $\epsilon=0.2$ (lower curve) and 0.5 (upper curve), with $\alpha=1$ and $d=0.1$. Calculated points are shown by solid circles.

The Néel temperatures calculated from Eq. (16) are 2.595, 2.110, and 1.746 for $\epsilon=1$, 0.5, and 0.2, respectively. The zero-point spin contractions Δ are 0.048, 0.055, and 0.067 for these respective values of ϵ, representing from about 10% to 13% of the spin magnitude. Figure 2 shows the layer magnetization versus temperature for $\epsilon=0.2$ and $\epsilon=0.5$.

B. $\epsilon\neq 1$, $\alpha\neq 1$

This is the most interesting case which corresponds to the binary antiferromagnetic superlattice with alternative layers of weak and strong interactions.

Figure 3 shows the layer magnetizations versus temperature T for $\alpha=1.5$ and 3, with $\epsilon=0.5$. Several interesting remarks are in order:

(i) The most striking feature is that at zero and low temperatures, the magnetization of the layer with stronger in-plane interaction (B layer) is smaller than that of the layer with weaker interaction (A layer). At first, it seems to be paradoxical, but this effect results from quantum fluctuations: Qualitatively, the stronger the *antiferromagnetic* interaction is, the smaller the magnetization will be, because the Néel antiferromagnetic ordering suffers more fluctuations. A similar effect has been observed in the case of antiferromagnetic thin films where the zero-point contraction of surface spins is smaller than that of inside layers,[18] and in the case of a frustrated system.[20]

(ii) At higher temperatures, there is a crossover between the two layer magnetizations: The stronger layer has the stronger magnetization. Quantum fluctuations are now dominated by thermal fluctuations.

(iii) The curvature of the magnetization of the weak layer depends rather sensitively on α. It can be concave, convex, or linear at high temperature. The self-consistent calculations, however, are very difficult near T_N for very

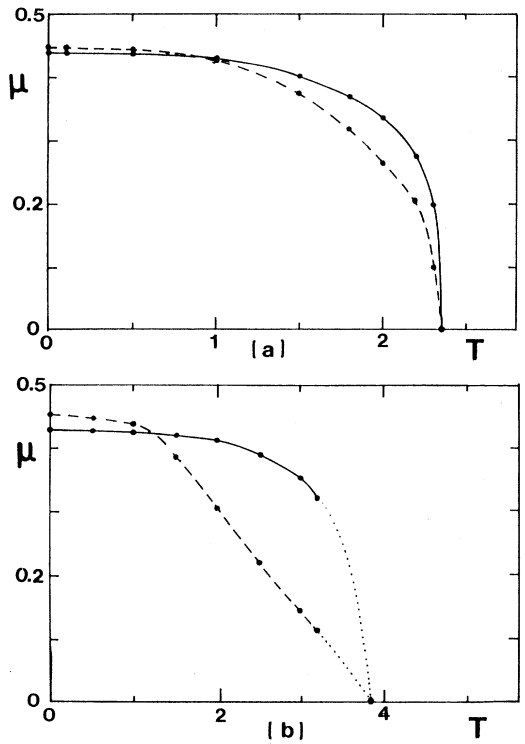

FIG. 3. Temperature dependence of magnetizations of A and B layers (dashed and solid curves, respectively) for $\epsilon=0.5$, $d=0.1$, and (a) $\alpha=1.5$, (b) $\alpha=3$. Calculated points are shown by solid circles, and dotted curves in (b) are extrapolations to the calculated Néel temperature.

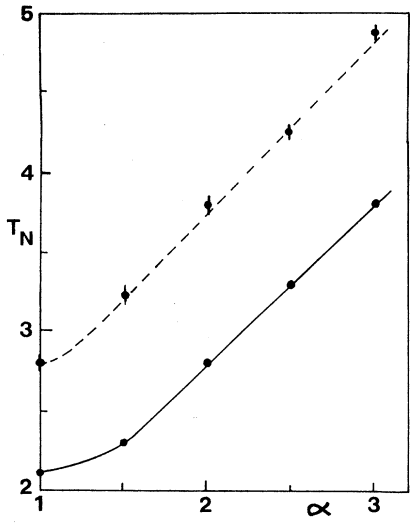

FIG. 4. Néel temperature T_N vs $\alpha=J_B/J_A$ obtained by Green-function method (solid curve) for $\epsilon=0.5$ and $d=0.1$. Results from Monte Carlo simulations of the corresponding classical Heisenberg spins of unit length are also shown (dashed curve) for comparison (see Sec. IV). Vertical bars indicate errors.

large α (Fig. 3).

It is noted that T_N is found between the values of Néel temperatures for two respective bulk materials. Figure 4 shows the Néel temperature versus α in the case $\epsilon=0.5$ and $d=0.1$ (solid curve). The results from our MC simulations (see Sec. IV) are also displayed (dashed curve) for comparison. Although for the simulations, classical Heisenberg spins of unit length have been used, the agreement between the two methods concerning the variation of T_N is remarkable. We will return to this point later.

C. Effect of anisotropy

Figure 5 shows the effects of the anisotropy d on T_N (solid curve, left scale) and on the layer magnetization (dashed curve, right scale) at $T=0$ in the case where $\alpha=1$ and $\epsilon=0.5$. The zero-point spin contraction decreases as d increases. When α is larger than 1, T_N increases strongly with increasing d. For example, when $\alpha=1.5$, $T_N=2.18$, 2.30, and 2.9 for $d=0.05$, 0.1, and 0.2, respectively.

IV. MONTE CARLO SIMULATION

In this section, we show the results from our MC simulations of the system described by Hamiltonian (1) but the spins are now classical with magnitude equal to 1.

The MC method used here for vector spins has been described in detail elsewhere.[21] We recall only briefly here: Multiflipping trial procedure was used and periodic boundary conditions were employed. The first 10^4 MC flipping trial steps per spin (MCS/spin) were discarded for equilibrating the system and the following 10^4 MCS/spin were used for averaging physical quantities. The lattice sizes used are $N=L^3$ with $L=8$, 10, 12, and 14, though the results shown in the following are for $L=14$ (the size effects are not significant for those sizes). Many independent runs with different random number sequences were performed to ensure the reproducibility of the results.

Figure 6 shows the internal energy per spin U as well as the specific heat per spin C calculated from the energy fluctuations, for a typical set of interactions $\epsilon=0.5$, $\alpha=1.5$, and $d=0.1$. The phase transition is recognized

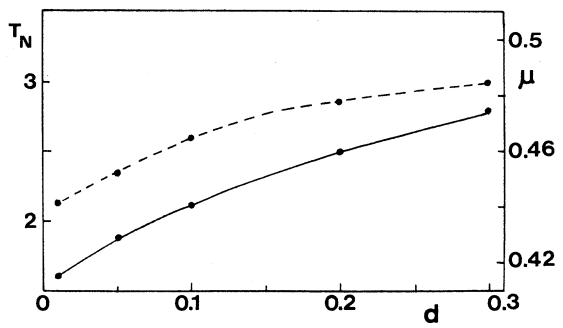

FIG. 5. T_N (solid curve, left scale) and layer magnetization μ at zero temperature (dashed curve, right scale) as functions of anisotropy d, for $\alpha=1$ and $\epsilon=0.5$.

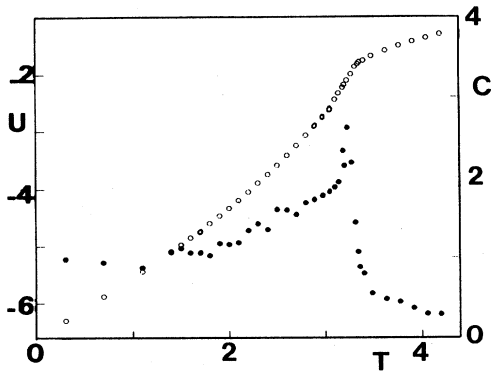

FIG. 6. Monte Carlo results for internal energy per spin U (open circles, left scale) and specific heat per spin C (solid circles, right scale) vs temperature T, for $\alpha=1.5$, $\epsilon=0.5$, and $d=0.1$.

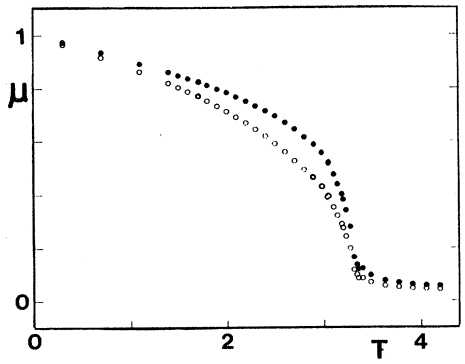

FIG. 7. Monte Carlo results for magnetizations per spin of A and B layers vs temperature T (open and solid circles, respectively), for $\alpha=1.5$, $\epsilon=0.5$, and $d=0.1$. As expected for classical spins, there is no crossover at low T as in the quantum case (see Fig. 3).

by the sharp peak of C associated with the change of curvature of U.

The layer magnetizations versus temperature are shown in Fig. 7. As expected for classical spins, the stronger layer has stronger magnetization at all temperatures, unlike the quantum case considered in Sec. III.

The Néel temperature as a function of α is shown in Fig. 4 together with that obtained from the Green-function method. One cannot compare the values of T_N of the two methods because of the difference of spin magnitudes used in the two methods. However, the variation of T_N with α is very similar.

V. CONCLUSION

The Green-function formalism for antiferromagnetic superlattices at finite temperatures presented in this paper can be easily generalized to study many other magnetic superlattices. Applications have been made to a few special cases. In particular, the case of binary antiferromagnetic superlattice has been studied. The results show several interesting effects at low temperatures which have no counterpart in ferromagnetic superlattices: zero-point spin contractions and the crossover of layer magnetizations at low temperatures due to quantum fluctuations. Monte Carlo simulations of the corresponding classical Heisenberg model have also been performed. The results show that the behavior of layer magnetization and the Néel temperature at high temperatures are in qualitative agreement with the quantum case.

ACKNOWLEDGMENTS

I would like to express my sincere thanks to Fundamental Research Laboratories of the NEC Corporation for hospitality and generous support of my stay. In particular, I am grateful to Dr. F. Saito, Dr. H. Watanabe, and Dr. S. Ohnishi for much help. I am also indebted to Miss Y. Chiba, Dr. S. Sawada, and Dr. S. Saito for their kindness, discussions, and help. Thanks are also due to Professor Satoru Sugano of the University of Tokyo for discussions and much help, and for providing me space at the Institute for Solid State Physics where part of this work has been done.

*On leave from Laboratoire de Magnétisme des Surfaces, Université Paris 7, 75251 Paris CEDEX 05, France.

[1]R. Du, F. Tsui, and C. P. Flynn, Phys. Rev. B **38**, 2941 (1988).
[2]N. Sato, J. Appl. Phys. **64**, 4113 (1988).
[3]L. Dobrzynski, B. Djafari-Rouhani, and H. Puszkarski, Phys. Rev. B **33**, 3251 (1986).
[4]A. Akjouj, B. Sylla, P. Zielinski, and L. Dobrzynski, Phys. Rev. B **37**, 5670 (1988).
[5]Q. Hong and T. H. Lin, Phys. Lett. A **124**, 181 (1987).
[6]Y. F. Zhou and T. H. Lin, Phys. Lett. A **134**, 257 (1989).
[7]D. Schwenk, F. Fishman, and F. Schwabl, Phys. Rev. B **38**, 11 618 (1988).
[8]R. E. Camley, T. S. Rahman, and D. L. Mills, Phys. Rev. B **27**, 261 (1983).
[9]P. Grunberg and K. Mika, Phys. Rev. B **27**, 2955 (1983); P. R. Emtage and M. R. Daniel, *ibid.* **29**, 212 (1984).
[10]B. Hillebrands, Phys. Rev. B **37**, 9885 (1988).
[11]L. L. Hinley and D. L. Mills, Phys. Rev. B **33**, 3329 (1986); **34**, 1698 (1986).
[12]C. Thibaudeau and A. Caillé, Phys. Rev. B **32**, 5907 (1987).
[13]C. Zhou and C. D. Gong, Phys. Rev. B **39**, 2603 (1989).
[14]E. C. Valadares and J. A. Plascak, Physica **A153**, 252 (1988).
[15]G. D. Pang and F. C. Pu, Phys. Rev. B **38**, 12649 (1988).
[16]J. Kanamori, *Magnetism I* (Academic, New York, 1963), p. 128.
[17]D. N. Zubarev, Usp. Fiz. Nauk. **71**, 71 (1960) [Sov. Phys. Usp. **3**, 320 (1960)].
[18]H. T. Diep, J. C. S. Levy, and O. Nagai, Phys. Status Solidi B **93**, 351 (1979).
[19]H. T. Diep, Phys. Status Solidi B **103**, 809 (1981).
[20]P. Azaria and H. T. Diep, J. Appl. Phys. **61**, 4422 (1987).
[21]H. T. Diep, Phys. Rev. B **39**, 397 (1989).